Numerical Assessment of Design Procedures for Overhanging Steel Girders

Vahab Esmaeili, Ali Imanpour, and Robert G. Driver

Abstract In the design of roof structures for large single-storey buildings, it is common practice to extend the primary girders of alternate bays beyond the columns to support the girders in the other bays, the span of which is adjusted to balance the moment distribution along the girder line. This structural system, typically with open-web steel joists constituting the secondary members, is commonly known as Gerber construction. Despite the common use of the Gerber system, concerns have arisen about how designers evaluate the stability of overhanging girders, as contemporary steel design standards remain mostly silent on how to take into account the interaction between the back span and the cantilever. The main objective of this paper is to provide new insights into the stability response and design of overhanging girders. Commonly used design procedures for overhanging girders used to assess the limit state of lateral–torsional buckling are first discussed. A finite-element model capable of considering material and geometric nonlinearities, residual stresses, initial out-of-straightness, and cross-sectional distortions is then utilised to obtain the buckling resistances of a practical range of overhanging girders. It is assumed that the back span is under top-flange loading, and open-web steel joists provide only lateral restraints to the main girder. Three different restraint conditions are considered at the cantilever tip: free, lateral restraint at the top flange, and lateral restraint at both the top and bottom flanges. Finally, the results are compared to the predictions of available design procedures. The results suggest that the current methods may lead to overly conservative or unconservative predictions, as they either overlook the role of interaction between the back span and the cantilever or miscalculate the beneficial effect of top-flange bracing on the stability of the back span under reverse-curvature bending.

Keywords Design procedures · Overhanging steel girders

V. Esmaeili (✉) · A. Imanpour · R. G. Driver
University of Alberta, Edmonton, AB, Canada
e-mail: vahab@ualberta.ca

1   Introduction

Cantilever-suspended-span construction, with overhanging girders considered to be the main components, is a popular roof framing scheme for large single-storey buildings in North America. The beauty of this system is that it enjoys more balanced moment distributions than its conventional counterpart with simply supported girders, thereby reducing the peak positive moments by allowing negative moments to develop at the column locations. In addition, simpler connections and ease of erection are among the comparative merits of such a structural system [2]. Nevertheless, a lack of consensus on the appropriate means of stability design of overhanging girders, considering the interaction between their individual segments, has consistently been a matter of concern among structural designers. There have also remained many unanswered questions on the way overhanging girders benefit from the restraints provided by the secondary members such as open-web steel joists (OWSJs).

In an effort to develop a design method for overhanging girders, [11] proposed the notional effective length concept, in which the back span and the cantilever segment are of the same length. The cantilever tip is assumed to be laterally restrained at the shear-centre level, whereas the back span is free of loads and restraints between the supports. The proposed method neglects to account for the effect of the back span bay dimension on the stability of the overhanging girder. In order to address this issue, [10] recommended considering the length of the back span as the minimum allowable effective length of the cantilever. However, the concept of effective length was adopted by the Structural Stability Research Council (SSRC) guide [8] without implementing the above-mentioned limitation.

An interaction method was proposed by [13] so as to obtain the elastic buckling resistance of a double-overhanging girder with equal cantilevers. It was assumed that the girder was unable to move laterally at the two supports. With regard to the loading condition at the cantilever tips, top-flange and shear-centre loadings were investigated. In this method, the buckling resistances of the back span and the cantilever are first estimated separately. The back span is assumed to be under a free-to-warp condition at the two ends, whereas the cantilever is considered built-in at the support. Eventually, the overall capacity of the double-overhanging girder is obtained considering the interaction between the adjacent segments. For the cases with top-flange loading at the tip, this method tends to overestimate the buckling resistance of the system [7].

Another interaction method was proposed by [7] in order to calculate the critical elastic moment of overhanging girders when the cantilever segment is more critical than the back span. It was assumed that no restraints were provided to the back span between the column locations. Additionally, both top-flange and shear-centre loadings were considered at the cantilever tip. In this method, the critical elastic moments associated with the individual segments under a free-to-warp condition at the supports are calculated. Interaction equations were provided for the cases with two different restraint conditions at the cantilever tip: free and laterally restrained

at the top-flange level. For the case where the cantilever tip is laterally restrained at both the top- and bottom- flange levels, the design procedures presented in the SSRC guide [8] or by [12] can be utilised. Furthermore, the overall buckling resistance of the overhanging girder can be taken as the buckling resistance of the back span if the back span is more critical [13].

The stability response of girders with reverse-curvature bending was investigated by [14] with the aim of finding the actual unbraced length of the girder with top-flange bracing under negative bending moments. It was recommended that the point of contraflexure could not generally be considered a braced point. Several lateral–torsional buckling (LTB) modification factors were also proposed to account for special cases of girders with reverse-curvature bending, including cases free between the supports and those with continuous bracing of the top flange. Furthermore, girders restrained at one flange were scrutinised, focusing on lateral and torsional bracings and composite construction.

Esmaeili et al. [6] further investigated the effect of top-flange bracing on the stability of girders with reverse-curvature bending, which are representative of the back span bay of a typical overhanging girder. The elastic buckling resistances associated with the back spans of 19,200 different single-overhanging girders with top-flange bracing under free-to-warp conditions were obtained through the finite-element method and compared to the predictions of prevailing design methods. The current LTB modification factors were found to be excessively either conservative or unconservative. An artificial intelligence (AI)-based model was also proposed for predicting the elastic buckling resistance of the back span of a typical single-overhanging girder with top-flange bracing under free-to-warp conditions.

From the presented literature review, it can be deduced that crucial questions have yet to be addressed in regard to the way current design methods account for the interaction buckling of overhanging girders and the actual effect of restraints afforded by secondary members. This paper is aimed at the performance assessment of commonly used design procedures for overhanging girders. To achieve this, a practical range of single-overhanging girders is first numerically simulated and analysed considering material and geometric nonlinearities as well as initial imperfections. The back span is assumed to be under top-flange loading, and only lateral restraints are considered to be provided to the girder by OWSJs. Also, three distinct restraint conditions are considered at the cantilever tip: free, lateral restraint at the top flange, and lateral restraint at both the top and bottom flanges. Finally, the results are compared to the predictions by current design procedures.

2 Scope of Numerical Simulations

Figure 1 depicts the configuration of a typical single-overhanging girder, along with its bending moment diagram, and presents the relevant load and geometric variables.
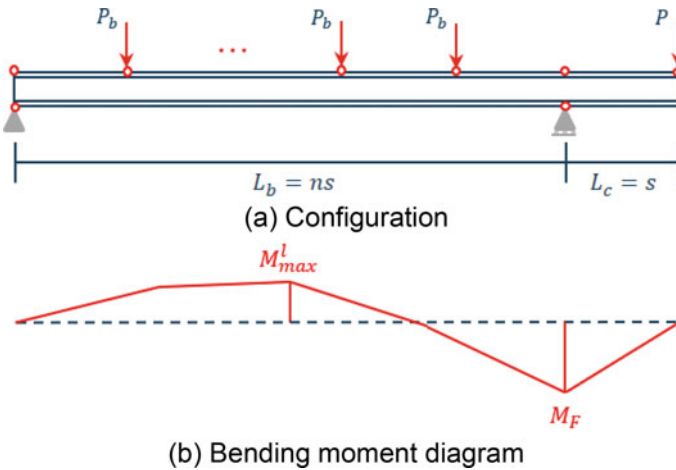
Fig. 1 Typical single-overhanging girder (symbol red circle represents point of lateral support)

In Fig. 1,

- P_b refers to the point loads on the back span arising from the end reactions of OWSJs;
- P represents the point load at the cantilever tip;
- L_b denotes the length of the back span;
- L_c is the length of the cantilever;
- s represents the joist spacing;
- n equals the number of point loads on the back span plus 1;
- M_{max}^l is the local maximum bending moment along the back span;
- M_F signifies the (negative) bending moment at the fulcrum;
- κ' is defined as the ratio between M_{max}^l and M_F, including sign.

A total of 1699 single-overhanging girders using 24 standard steel W-shapes, representing the most common cross-sections utilised in Gerber construction, are considered. The selected sections conform to CSA G40.21 Grade 345WM [4], which is aligned with ASTM A992 [1]. The W-shapes considered, along with the class of each [5], are presented in Table 1.

Herein lies the main modelling features:

- Lateral deflections and twisting are prevented at support locations (fork supports).
- Warping deformation is allowed at support locations.
- Torsional restraints afforded to the girder by OWSJs are neglected.
- Restraints afforded and loads delivered to the girder by OWSJs are defined as follows:

    – For the back span, loads and lateral restraints are applied at the top-flange level.

Table 1 W-shapes considered and classes of cross-sectional elements

Cross section	Class		Cross section	Class		Cross section	Class	
	Flange	Web		Flange	Web		Flange	Web
W410 × 39	2	2	W530 × 82	2	1	W690 × 152	1	1
W410 × 60	1	1	W530 × 138	1	1	W760 × 134	2	2
W410 × 85	1	1	W610 × 92	1	1	W760 × 147	1	1
W460 × 52	1	1	W610 × 125	1	1	W760 × 161	1	1
W460 × 60	1	1	W610 × 155	2	1	W840 × 176	1	1
W460 × 97	1	1	W610 × 241	1	1	W840 × 193	1	1
W460 × 144	1	1	W690 × 125	1	1	W920 × 201	1	1
W530 × 66	1	1	W690 × 140	1	1	W920 × 223	1	1

- Three different restraint conditions are considered at the cantilever tip: (1) free, (2) lateral restraint at the top flange—as shown in Fig. 1—and (3) lateral restraint at both top and bottom flanges.
- For restraint condition (1), the point load at the cantilever tip comes from the adjacent drop-in segment and is applied at the shear-centre level.
- For restraint conditions (2) and (3), the point load at the cantilever tip comprises both joist and drop-in segment reactions and is conservatively applied at the top-flange level.

Considering the above-mentioned criteria, Table 2 summarises all the possible loading and restraint conditions (LRCs) considered, and Fig. 2 depicts the three configurations.

To illuminate the inclusiveness and practicality of the set of girders considered, the statistical indices associated with the contributing variables are reported in Table. Figures 3 and 4 demonstrate the relative frequency distribution for the length of back span and joist spacing, along with their mean values and coefficients of variation.

In Table 3,

- $\frac{b}{2t}$ signifies the flange slenderness ratio, where b is the overall width of the flange and t denotes its thickness;
- $\frac{h}{w}$ is indicative of the web slenderness, where h denotes the clear depth of the web and w is its thickness;

Table 2 Loading and restraint conditions (LRCs)

		Cantilever tip	
		Restraint condition	Loading condition
	LRC 1	Condition (2)	Top flange
	LRC 2	Condition (1)	Shear centre
	LRC 3	Condition (3)	Top flange

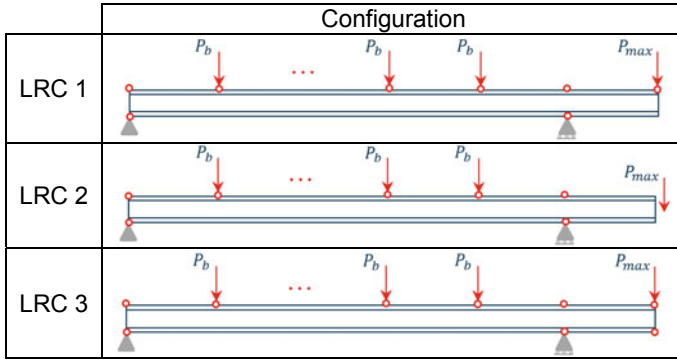| Configuration	
LRC 1	
LRC 2	
LRC 3	

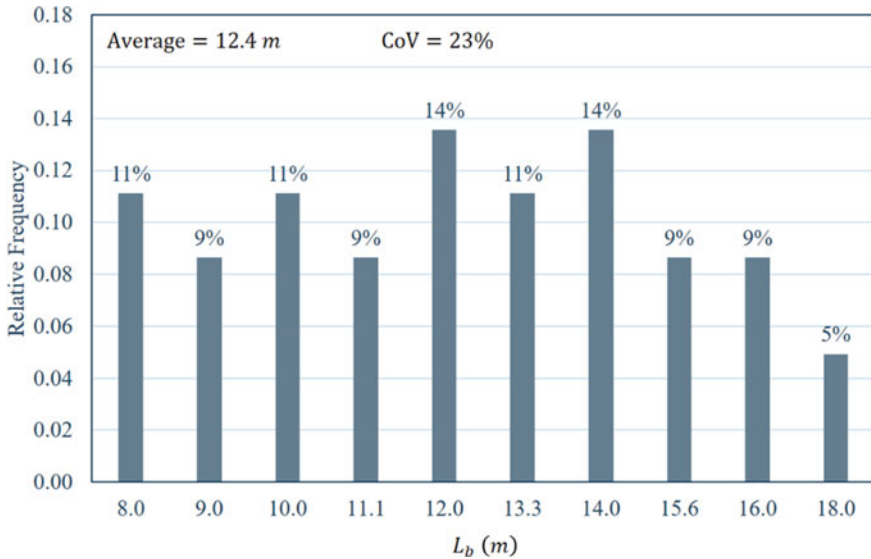**Fig. 2** Configurations for single-overhanging girders

Fig. 3 Relative frequency distribution for length of back span, L_b

- $\frac{I_x}{I_y}$ represents the ratio of the strong- and weak-axis geometric stiffnesses of the girder;
- $\frac{d}{b}$ is the overall cross-sectional aspect ratio of the girder, where d is the depth of the section and b is the width of the flange;
- $X = \frac{\pi}{L_b}\sqrt{\frac{EC_w}{GJ}}$ is principally a torsional parameter reflective of the ratio between the warping and St. Venant torsional stiffnesses;
- $\frac{L_b}{d}$ is the ratio between the length of the back span and the overall depth of the section;
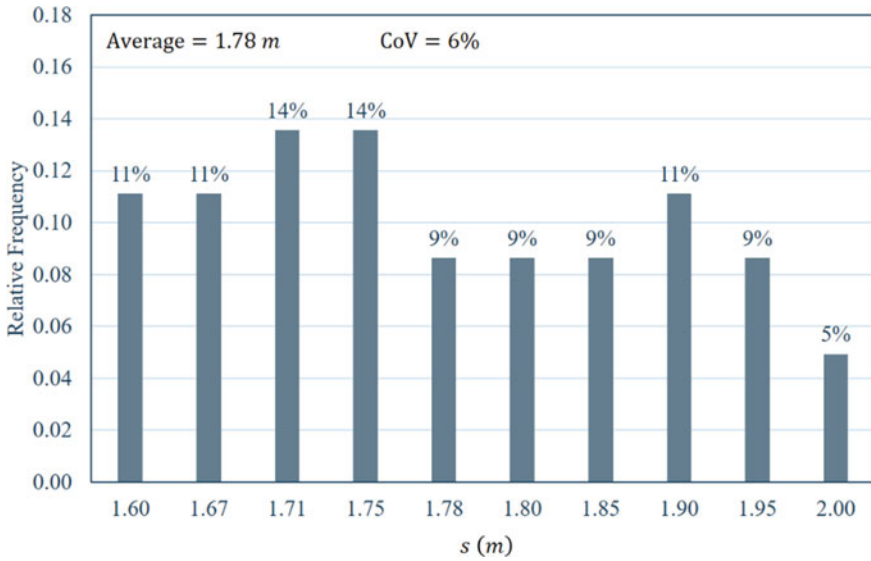
Fig. 4 Relative frequency distribution for joist spacing, s

Table 3 Statistical indices associated with the contributing variables

	$L_b(m)$	$s(m)$	$\frac{b}{2t}$	$\frac{h}{w}$	$\frac{I_x}{I_y}$	$\frac{d}{b}$	X	$\frac{L_b}{d}$	$\frac{L_b}{r_y}$
Maximum	18.0	2.00	8.5	60.4	45.2	3.4	1.1	22	347
Minimum	8.0	1.60	4.5	31.5	8.7	1.7	0.4	15	119
Mean	12.4	1.78	6.8	49.7	27.1	2.7	0.7	19	240
Coefficient of variation (CoV) (%)	23	6	16	18	33	15	18	10	21

- $\frac{L_b}{r_y}$ is the ratio between the length of the back span and the radius of gyration of the section about its weak axis.

It is important that a broad variety of load patterns be considered in the evaluation of the existing design procedures. To establish a criterion for measuring this factor, a typical roof framing under a schematic load pattern is considered—as shown in Fig. 5.
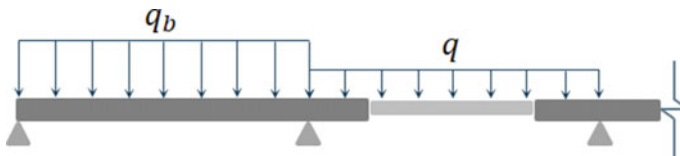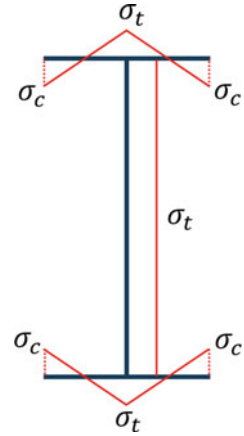

Fig. 5 Typical roof framing under a schematic load pattern

Fig. 6 Residual stress
pattern proposed by
Galambos and Ketter [9]

In Fig. 5, q_b refers to the intensity of the uniformly distributed load on the back span bay; q represents the uniformly distributed load on the adjacent bay; and κ'' is defined as the ratio between q_b and q. To ensure that the dataset includes the most commonly used load patterns, the following range is considered for κ'':

$$\kappa'' = \{2.00, 1.60, 1.30, 1.00, 0.77, 0.63, 0.50\} \tag{1}$$

For the purpose of numerical simulation, the finite-element model developed by [6]—which is capable of considering material and geometric nonlinearities and imperfections—is adopted. An elastic–perfectly plastic stress–strain curve is considered for the material with an elastic modulus and a yield stress of 200 GPa and 345 MPa, respectively. Moreover, a parabolic sweep with the maximum out-of-straightness of $L_b/1000$ along the back span is used to introduce initial geometric imperfections into the numerical model. In order for the residual stresses to be incorporated, the pattern proposed by Galambos and Ketter [9]—as shown in Fig. 6—is employed.

In Fig. 6,

- $\sigma_c = 0.3F_y$ represents the maximum compressive stress at the flange tips, where F_y signifies the specified minimum yield stress of steel;
- $\sigma_t = \frac{bt}{bt+w(d-2t)}\sigma_c$ is the maximum tensile stress throughout the web and at the flange-web intersection.

To distinguish between various types of instability, the maximum internal bending moment, the maximum compressive stress, and deformations throughout the girder are monitored during analysis. Therefore, if no local instabilities are captured, three different scenarios are possible:

- The girder becomes unstable as a result of plastic hinge formation as soon as the maximum internal bending moment reaches the plastic moment of the section, M_p.

- The instability of the girder is classified as inelastic buckling if the compression flange is partly yielded at the buckling stage.
- The instability of the girder is classified as elastic buckling if the compression flange is not yielded at the buckling stage.

3   Existing Design Methods

For the design of overhanging girders, it is standard practice to first obtain the buckling resistances of their individual segments, i.e. the back span and the cantilever segment, separately. Afterwards, the buckling resistance of the entire system is calculated either considering or neglecting the interaction between the individual segments.

3.1   Back Span

The back span of overhanging girders typically experiences both positive and negative bending moments. Considering the different bracing conditions at the top and bottom flanges along the back span, its adequacy under these two moments needs to be evaluated in different ways.

3.1.1   Under Maximum Positive Moment

The capacity of the back span under the maximum positive moment can be checked based on the procedure CSA S16-19 (2019) proposes for the bending capacity of laterally unsupported members. To do this, the critical elastic moment of the back span at the point of maximum positive moment is calculated as:

$$M_{cr_b}^+ = \frac{\omega_2 \pi}{s} \sqrt{E I_y G J + \left(\frac{\pi E}{s}\right)^2 I_y C_w} \tag{2}$$

where E and G are the elastic modulus and shear modulus of steel, respectively; I_y is the moment of inertia about the weak axis of the cross section; J and C_w represent the St. Venant torsional constant and warping torsional constant, respectively; s is the joist spacing representing the unbraced length as the top flange is under compression; and ω_2 is a coefficient to account for various moment gradients along the unbraced segment and is calculated using the following equation:

$$\omega_2 = \frac{4M_{\max}}{\sqrt{M_{\max}^2 + 4M_a^2 + 7M_b^2 + 4M_c^2}} \leq 2.5 \tag{3}$$

In Eq. (3), M_a, M_b, and M_c are the absolute values of moments at the quarter point, centreline, and three-quarter point of the unbraced segment, respectively; $M_{\max}$ is the absolute value of the maximum moment in the unbraced segment.

3.1.2 Under Maximum Negative Moment

The capacity of the back span under the maximum negative moment can be evaluated in two different ways. The first approach is to use the same procedure as for the back span under the maximum positive moment, considering the full length of the back span as the unbraced length. Therefore, the critical elastic moment of the back span at the point of maximum negative moment is calculated as:

$$M_{cr_b}^{-} = \frac{\omega_2 \pi}{L_b} \sqrt{EI_y GJ + \left(\frac{\pi E}{L_b}\right)^2 I_y C_w} \tag{4}$$

where L_b is the length of the back span. The reason that L_b is considered to be the unbraced length is that the bottom flange is partly under compression, but no lateral restraints are provided to the bottom flange between the two supports. Additionally, the point of contraflexure—where the bending moment is zero—could not generally be considered a point of lateral support.

The second approach is to replace ω_2 with an LTB modification factor proposed by [14], which is calculated as:

$$C_{b-\text{YH}} = 3.0 - \frac{2}{3}\left(\frac{M_1}{M_o}\right) - \frac{8}{3}\left[\frac{M_{CL}}{(M_o + M_1)}\right] \tag{5}$$

in which M_o is the (negative) moment at the end of the back span that gives the largest compressive stress in the bottom flange; M_1 is the moment at the other end of the back span; M_{CL} is the moment at the centreline of the back span, including sign; and $(M_o + M_1)$ is taken equal to M_o if M_1 is positive and causes tension on the bottom flange.

3.2 Cantilever

In order to check the adequacy of the cantilever segment, the notional effective length—as defined by [10]—is utilised. In this approach, the critical elastic moment of the cantilever segment—under its actual loading and restraint conditions—is assumed to be equal to that of a notional simply supported girder of identical section under uniform moment. Thus, the critical elastic moment of the cantilever is calculated as:

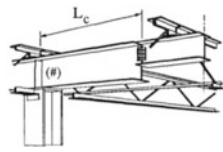$$M_{cr_c} = \frac{\pi}{kL_c}\sqrt{EI_yGJ + \left(\frac{\pi E}{kL_c}\right)^2 I_y C_w}$$ (6)
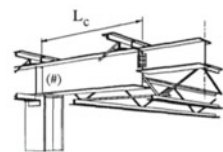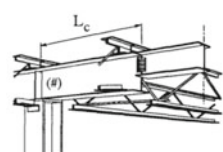
where L_c signifies the length of the cantilever; k is referred to as effective length factor and is determined based on the loading and restraint conditions of the cantilever, as presented in Table 4.

A different set of effective length factors was proposed by the Canadian Institute of Steel Construction [2] as specified in Table 5.

Table 4 Effective length factors, k, proposed by [10]

Restraint condition	Loading condition at tip	
	Top flange	Others
	2.5	1.0
	2.5	0.9
	1.2	0.7

Table 5 Effective length factors, k, proposed by the CISC [2]

Condition[a]	Restraints	k
		1.5–2.5
		1.0–1.5
		0.8–1.0

[a] Lateral restraint is provided to bottom flange at the root of cantilever by OWSJ bottom chord extension

3.3 Interaction Method

For an overhanging girder, due to the interaction between its adjacent segments during buckling, the less critically loaded segment restrains the more critically loaded one [7]. When the back span is more critical, the overall buckling resistance of the overhanging girder can be taken as the buckling resistance of the back span alone [13]. However, when the cantilever is more critical and its tip is either free or laterally restrained at the top-flange level only, the critical elastic moment of the overhanging girder at the point of maximum negative moment is determined as [7]:

$$M_{\mathrm{cr}}^- = M_{\mathrm{cr}_c} + F_I \big(M_{\mathrm{cr}_b}^- - M_{\mathrm{cr}_c} \big) \tag{7}$$

where

- $M_{\mathrm{cr}_b}^-$ refers to the critical elastic moment of the back span at the point of maximum negative moment and can be calculated based on Eq. (4) through either ω_2 (Eq. 3) or $C_{b-\mathrm{YH}}$ (Eq. 5);
- M_{cr_c} denotes the critical elastic moment of the cantilever at the point of maximum negative moment and is calculated as specified in Table 6;
- F_I is referred to as interaction factor and is calculated as specified in Table 7.

For the case where lateral restraints are provided to both the top and bottom flanges at the cantilever tip, the following steps need to be taken [12]:

- The critical elastic moment of the cantilever is calculated as:

$$M_{\mathrm{cr}_c} = \frac{1.75\pi}{L_c} \sqrt{E I_y G J + \left(\frac{\pi E}{L_c} \right)^2 I_y C_w} \tag{8}$$

- The stiffness of the back span, the restraining segment, is defined as:

Table 6 Critical elastic moment of cantilever segment, M_{cr_c} [7]

Loading condition	M_{cr_c}
Top flange	$1.5 \frac{GJ}{d}$
Shear centre	$\frac{4}{L_c} \sqrt{E I_y G J}$

Table 7 Interaction factors, F_I, proposed by [7]

Restraint condition	Interaction factor (F_I)
	$-0.08 + 0.18 \frac{L_b}{L_c} - 0.009 \left(\frac{L_b}{L_c} \right)^2$
	$0.064 + 0.162 \frac{L_b}{L_c} - 0.009 \left(\frac{L_b}{L_c} \right)^2$

$$\alpha_b = \frac{3EI_y}{L_b}\left(1 - \frac{M_{cr_c}}{M_{cr_b}^-}\right) \tag{9}$$

- The stiffness of the cantilever, the critical segment, is computed as:

$$\alpha_c = \frac{3EI_y}{L_c} \tag{10}$$

- The stiffness ratio for the root of the cantilever is calculated as:

$$G_{Root} = \frac{\alpha_c}{\alpha_b} \tag{11}$$

- Assuming infinity as the stiffness ratio for the cantilever tip, G_{Tip}, implying it is free to rotate about the weak axis and warp, the effective length factor for interaction method—k_I—is determined from Fig. 7.
- Using the following equation, the critical elastic moment of the overhanging girder at the point of maximum negative moment is obtained:

Fig. 7 Nomograph for effective length factors of columns in continuous frames with sidesway prevented [3]
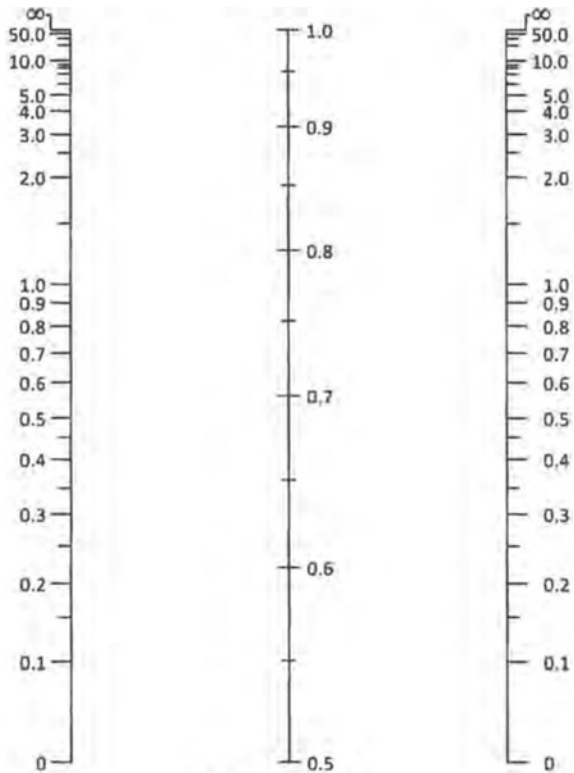
$$M_{\text{cr}}^- = \frac{1.75\pi}{k_I L_c} \sqrt{E I_y G J + \left(\frac{\pi E}{k_I L_c}\right)^2 I_y C_w} \tag{12}$$

3.4 Ultimate Capacity

Having the critical elastic moments of the individual segments, the following steps are taken to finalise the design:

- M_{cr}^+, the critical elastic moment of the overhanging girder at the point of maximum positive moment, is set to $M_{\text{cr}_b}^+$ (Eq. 2).
- For methods considering the interaction between the back span and the cantilever, M_{cr}^-—the critical elastic moment of the overhanging girder at the point of maximum negative moment—is obtained from Eqs. (7) or (12) based on the restraint condition at the cantilever tip.
- For methods neglecting the interaction between the back span and the cantilever, M_{cr}^- is taken as the lesser of $M_{\text{cr}_b}^-$ and M_{cr_c}.
- M_n^+, the nominal capacity of the overhanging girder at the point of maximum positive moment, is determined as [5]:

$$M_n^+ = \begin{cases} M_{\text{cr}}^+ & M_{\text{cr}}^+ \le 0.67 M_p \\ 1.15 M_p \left[1 - \frac{0.28 M_p}{M_{\text{cr}}^+}\right] \le M_p & M_{\text{cr}}^+ > 0.67 M_p \end{cases} \tag{13}$$

- M_n^-, the nominal capacity of the overhanging girder at the point of maximum negative moment, is calculated as [5]:

$$M_n^- = \begin{cases} M_{\text{cr}}^- & M_{\text{cr}}^- \le 0.67 M_p \\ 1.15 M_p \left[1 - \frac{0.28 M_p}{M_{\text{cr}}^-}\right] \le M_p & M_{\text{cr}}^- > 0.67 M_p \end{cases} \tag{14}$$

- M_n, the overall nominal capacity of the overhanging girder, is then computed as:

$$M_n = \begin{cases} M_n^- & \frac{M_n^+}{M_n^-} \ge |\kappa'| \\ \frac{M_n^+}{|\kappa'|} & \frac{M_n^+}{M_n^-} < |\kappa'| \end{cases} \tag{15}$$

It is noteworthy that M_n is nominally the maximum moment the overhanging girder can resist at the location of maximum negative moment, that is, the fulcrum.

4 Performance Assessment of Existing Design Procedures

Based on the design methods utilised for checking the adequacy of the individual segments of the overhanging girder and the decision as to whether or not the interaction between the individual segments is to be taken into account, the designer could adopt any of the design procedures presented in Table 8.

In order to evaluate the performance of the above-mentioned design procedures, for each girder from the 1,699 cases previously defined for the numerical simulation, the nominal capacity—taken at the fulcrum—is obtained from a finite-element analysis (FEA) and introduced as $M_{n-\text{FEA}}$. The nominal capacity of each case is also calculated based on the six design procedures specified in Table 8. Afterwards, the performance of each design procedure is evaluated for each of the LRCs of single-overhanging girders through the information summarised in Tables 9 and 10. In Table 9, the mean normalised moments for each of the LRCs of single-overhanging girders obtained from the FEAs are presented. Additionally, the mean ratio between the nominal capacities obtained from the FEAs and those calculated using each of the six design procedures specified in Table 8 is reported in Table 10—along with the associated coefficient of variation—for each type of instability separately.

From Tables 9 and 10, the following observations emerge:

- Under LRC 1,
  - a few girders (4.4%) buckle elastically;
  - the mean value of $\frac{M_{\text{max}-\text{FEA}}}{M_p}$ is equal to 0.80—representing a quite inclusive range of girders that undergo inelastic buckling;

Table 8 Existing design procedures for overhanging girders

Procedure		$M_{\text{cr}_b}^+$	$M_{\text{cr}_b}^-$	M_{cr_c} or M_{cr}^-
1	S16/S16/IM	S16-19 (2019)	S16-19 (2019)	Interaction method
2	S16/YH/IM	S16-19 (2019)	[14]	Interaction method
3	S16/S16/KN	S16-19 (2019)	S16-19 (2019)	[10]
4	S16/S16/CISC	S16-19 (2019)	S16-19 (2019)	CISC [2]
5	S16/YH/KN	S16-19 (2019)	[14]	[10]
6	S16/YH/CISC	S16-19 (2019)	[14]	CISC [2]

Table 9 Mean normalised moments for different LRCs based on FEAs

	$\left(\frac{M_{n-\text{FEA}}}{M_p}\right)_{\text{mean}}$	$\left(\frac{|\kappa'|M_{n-\text{FEA}}}{M_p}\right)_{\text{mean}}$	$\left(\frac{M_{\text{max}-\text{FEA}}}{M_p}\right)_{\text{mean}}^{\text{a}}$
LRC 1	0.49	0.73	0.80
LRC 2	0.61	0.85	0.94
LRC 3	0.66	0.88	0.98

[a] $M_{\text{max}-\text{FEA}} = \max\left(M_{n-\text{FEA}}, |\kappa'|M_{n-\text{FEA}}\right)$

Table 10 FEA/design ratios for existing design procedures

LRC 1

Instability type		Elastic		Inelastic		Plastic	
Number of cases		25		427		115	
Procedure		Mean	CoV (%)	Mean	CoV (%)	Mean	CoV (%)
1	S16/S16/IM	1.52	26	1.86	26	1.24	23
2	S16/YH/IM	0.83	11	0.82	17	1.00	0
3	S16/S16/KN	1.26	33	1.70	28	1.19	22
4	S16/S16/CISC	1.26	33	1.70	28	1.19	22
5	S16/YH/KN	0.81	15	0.82	19	1.00	0
6	S16/YH/CISC	0.64	8	0.79	21	1.00	0

LRC 2

Instability type		Elastic		Inelastic		Plastic	
Number of cases		9		353		204	
Procedure		Mean	CoV (%)	Mean	CoV (%)	Mean	CoV (%)
1	S16/S16/IM	1.88	23	2.29	35	1.46	37
2	S16/YH/IM	1.01	5	0.98	4	1.01	3
3	S16/S16/KN	1.88	23	2.29	35	1.46	37
4	S16/S16/CISC	1.88	23	2.29	35	1.46	37
5	S16/YH/KN	1.01	5	0.98	4	1.01	3
6	S16/YH/CISC	1.02	4	0.98	5	1.01	3

LRC 3

Instability type		Elastic		Inelastic		Plastic	
Number of cases		0		301		265	
Procedure		Mean	CoV	Mean	CoV (%)	Mean	CoV (%)
1	S16/S16/IM	–	–	2.48	43	1.76	45
2	S16/YH/IM	–	–	1.05	14	1.04	7
3	S16/S16/KN	–	–	2.48	43	1.76	45
4	S16/S16/CISC	–	–	2.48	43	1.76	45
5	S16/YH/KN	–	–	1.05	14	1.04	7

Table 10 (continued)

LRC 3							
Instability type		Elastic		Inelastic		Plastic	
Number of cases		0		301		265	
Procedure		Mean	CoV	Mean	CoV (%)	Mean	CoV (%)
6	S16/YH/CISC	–	–	1.05	14	1.04	7

- the accuracy of the considered design procedures mostly depends on the method used for the calculation of $M_{\mathrm{cr}_b}^-$;
- the procedures using the S16 method to calculate $M_{\mathrm{cr}_b}^-$ tend to be overly conservative;
- in the procedures using the S16 method to calculate $M_{\mathrm{cr}_b}^-$ without considering the interaction between the back span and the cantilever, M_{cr_c} can never affect the ultimate capacity of the overhanging girder owing to the conservatism of the S16 method;
- the procedures using $C_{b-\mathrm{YH}}$ to calculate $M_{\mathrm{cr}_b}^-$ tend to be unconservative—yet practically accurate for the cases reaching their fully plastic capacity;
- considering the interaction between the back span and the cantilever could make the design procedure even more conservative when the S16 method is employed to calculate $M_{\mathrm{cr}_b}^-$;
- using the CISC's effective length factors rather than Kirby and Nethercot's to calculate M_{cr_c} could make the design procedure even more unconservative when $C_{b-\mathrm{YH}}$ is utilised to calculate $M_{\mathrm{cr}_b}^-$.

- Under LRC 2,

  only a very few girders (1.6%) experience elastic buckling;
  the mean value of $\frac{M_{\mathrm{max-FEA}}}{M_p}$ is quite close to 1.0—which means, for the cases going under inelastic buckling, very large portions of the most critical compression flanges yielded;
  the accuracy of the design procedures solely depends on the method used for the calculation of $M_{\mathrm{cr}_b}^-$;
  the procedures using the S16 method to calculate $M_{\mathrm{cr}_b}^-$ tend to be overly conservative—i.e. more conservative than those under LRC 1;
  the procedures using $C_{b-\mathrm{YH}}$ to calculate $M_{\mathrm{cr}_b}^-$ are sometimes unconservative—yet quite accurate.

- Under LRC 3,

  none of the girders undergoes elastic buckling;
  the mean value of $\frac{M_{\mathrm{max-FEA}}}{M_p}$ is practically equal to 1.0—which means even the cases experiencing inelastic buckling tend to verge on plastic hinge formation;
  the accuracy of the design procedures solely depends on the method used for the calculation of $M_{\mathrm{cr}_b}^-$;

the procedures using the S16 method to calculate $M_{\mathrm{cr}_b}^-$ tend to be overly conservative—i.e. more conservative than those under LRC 2;

the procedures using $C_{b-\mathrm{YH}}$ to calculate $M_{\mathrm{cr}_b}^-$ are mostly unconservative—yet quite accurate.

5   Summary and Conclusions

A set of 1699 single-overhanging girders was analytically investigated considering material and geometric nonlinearities, residual stresses, initial geometric imperfections, and cross-sectional distortions. As a result of open-web steel joists, the concentrated loads and lateral restraints were applied at the top-flange level—at discrete locations along the back span. Three different restraint conditions were considered at the cantilever tip: free, lateral restraint at the top flange, and lateral restraint at both the top and bottom flanges. The results reveal that existing design procedures may lead to overly conservative or unconservative predictions, as a result of neglecting the interaction between the back span and the cantilever or miscalculating the effect of top-flange bracing on the stability of the back span under reverse-curvature bending. Furthermore, the level of conservatism could differ significantly for different loading and restraint conditions at the cantilever tip, as well as different potential types of instability. It can also be concluded that the method used for calculating the critical elastic moment of the back span at the point of maximum negative moment could dramatically affect the accuracy of the design procedure.

References

1. American Society for Testing and Materials (ASTM) (2020) Standard specification for structural steel shapes. ASTM A992/A992M-20, ASTM, West Conshohocken, Pennsylvania, USA
2. Canadian Institute of Steel Construction (CISC) (1989) Roof framing with cantilever (gerber) girders and open-web steel joists. CISC, Markham, Ontario, Canada
3. Canadian Institute of Steel Construction (CISC) (2017) Handbook of steel construction, 11th edn. CISC, Markham, Ontario, Canada

4. Canadian Standards Association (CSA) (2013) General requirements for rolled or welded structural quality steel/structural quality steel. CSA G40.20-13/G40.21-13 (reaffirmed 2018), CSA, Toronto, Ontario, Canada
5. Canadian Standards Association (CSA) (2019) Design of steel structures. CSA S16-19, CSA, Toronto, Ontario, Canada
6. Esmaeili V, Imanpour A, Driver RG (2021) Stability of gerber systems with top-flange bracing. In: Proceedings of the annual stability conference. Structural Stability Research Council (SSRC). Louisville, Kentucky, USA
7. Essa HS, Kennedy DJL (1994) Design of cantilever steel beams: refined approach. J Struct Eng 120(9):2623–2636
8. Galambos TV (1998) Guide to stability design criteria for metal structures. Structural Stability Research Council (SSRC), Wiley, New York, USA
9. Galambos TV, Ketter RL (1959) Columns under combined bending and thrust. J Eng Mech Div 85(2):1–30
10. Kirby PA, Nethercot DA (1979) Design for structural stability. In: Constrado Nomographs. Granada Publishing, London, United Kingdom
11. Nethercot DA (1973) The effective lengths of cantilevers as governed by lateral buckling. Struct Eng 51(5):161–168
12. Schmitke CD, Kennedy DJL (1985) Effective lengths of laterally continuous, laterally unsupported steel beams. Can J Civ Eng 12(3):603–616
13. Trahair NS (1983) Lateral buckling of overhanging beams. In: Instability and plastic collapse of steel structures. Granada Publishing, London, United Kingdom
14. Yura JA, Helwig TA (2010) Buckling of beams with inflection points. In: Proceedings of the annual stability conference. Structural Stability Research Council (SSRC), Orlando, Florida, USA, 761–780